An Ultrasonic Osteotomy Device Enhanced Post-osteotomy Bone Healing Beyond That With a Conventional Rotary Device in a Rat Calvarial Model

Atsushi Danjo (danjoat@cc.saga-u.ac.jp)
Saga University
Reona Aijima
Saga University
Reiko U.Yoshimoto
Saga University
Shin-Ichi Tanaka
Nakanishi Inc
Takeshi Katsuki
Saga University
Mizuho A.Kido
Saga University
Yoshio Yamashita
Saga University

Research Article

Keywords: piezosurgery, bone regeneration, histology, micro-CT, animal study

Posted Date: January 15th, 2021

DOI: https://doi.org/10.21203/rs.3.rs-144269/v1

Version of Record: A version of this preprint was published at Journal of Oral and Maxillofacial Surgery, Medicine, and Pathology on January 1st, 2022. See the published version at https://doi.org/10.1016/j.ajoms.2021.10.002.

Abstract

Ultrasonic osteotomy devices (UODs) have many clinical benefits; for example, they cause little damage to adjacent tissues in oral surgery. However, few reports have focused on bone healing with UODs. This study aimed to compare bone healing after osteotomy with UODs versus rotary osteotomy devices (RODs) in a rat calvarial defect model. Calvarial bone defects were made with a UOD on the right side and an ROD on the left side. Micro-CT analysis revealed that the bone volume was greater with a UOD than with an ROD at 2-3 weeks. In HE-stained sections and micro-CT images, the bone wound gap was closed earlier on the UOD side than on the ROD side. Bone thickness, the quantity of newly formed bone, and the number of osteocytes were greater on the UOD side than on the ROD side. Scanning electron microscopy (SEM) showed that UOD cuts had smoother surfaces than ROD cuts. Osteoblast-like cells harvested from bone chips cut by the UOD had greater proliferative activity than those harvested from ROD-cut bone chips. The use of a UOD may assist bone regeneration, presumably because of osteoblast activation by ultrasonic microvibration and UODs cause less damage to the bone than RODs.

Introduction

Several bone modulation technologies have been developed recently, such as electric, ultrasonic (piezoelectric), and laser devices. Bone cutting and harvesting constitute one of the most common procedures in craniofacial surgeries, which include bone grafting and implant surgery. The usual bone cutting instruments are electric or air-powered saws with a sharp rotating or reciprocating blade. Recently, a bone cutting device using ultrasonic vibration has been utilized for oral surgery. Surgical treatment must always minimize pain and additional tissue damage, prevent infection, and promote rapid healing without complications. Conventional rotary osteotomy devices (RODs) have a long history in dental clinics and are powerful tools because they can cut bone rapidly, enabling a short operation time. Ultrasonic devices have been in general use for oral surgery since they were developed by Vercelloti in 1988. Ultrasonic osteotomy devices (UODs) have been designed to cut mineralized bone selectively using ultrasonic waves, which enables osteotomy to be performed with little soft tissue damage [1]. In addition, wisdom tooth extraction with UOD was associated with less postoperative swelling, pain, and trismus than extraction with a round burr on the other side [2]. Additionally, operations using UODs are favoured for their easier perioperative management, a result of the small volume of blood loss, in temporomandibular joint reconstruction [3] and vertebral canal operations [4]; additionally, there is little occurrence of neuropathy in sagittal splitting ramus osteotomy [5]. Despite these attractive advantages, UODs have not been generally used in dental practice because they require a longer cutting time than ROD. Furthermore, the topological and chronological differences of regenerating tissues after ROD and UOD cutting have not been clearly demonstrated. There are controversial studies regarding the effect of ROD and UOD cutting. In dog mandibular marginal resection models, Vercellotti et al. [6] reported that tissues cut by a UOD showed more bone formation than those cut by conventional ROD. It has been reported that ultrasonic irradiation of bone defects promotes cell growth and enhances bone regeneration

[7]. On the other hand, Ma et al. [8] did not observe distinct histological differences in the bone healing process between UODs and RODs.

To address the difference in tissue response of bone defects between UOD cuts and ROD cuts, we utilized the rat split model to minimize differences among individuals. We evaluated the early (1 and 4 weeks) osseous healing responses using radiographic three-dimensional analyses, histological approaches, and bone regenerating capacity by in vitro culture.

Results

The UOD took longer than the ROD but produced a finer calvarial cutting surface

None of the rats showed any remarkable postoperative complications or signs of distress throughout the 4-week experimental period. The UOD required a significantly longer time (average 66.6 sec) to cut the calvarial bone, approximately 2.8 times longer than the ROD (average 23.9 sec) (Fig. 1A). SEM observations revealed a smooth cutting surface without micro-fractures at the UOD sites and a rough and inward-curled bone surface with micro-fractures and smears at the ROD sites (Fig. 1B).

UOD sites gained more bone volume than ROD sites

In order to evaluate bone regeneration after osteotomy, bone morphology and X-ray intensity were observed by micro-CT every week from day 0 to 4 weeks. On day 0, no differences were observed in the size of the bone defect (Fig. 1C). After 2 weeks, at UOD sites, the reconstructed X-ray images showed regenerated tissues protruding towards the bone defect space, and the defect was smaller than the corresponding one on the opposite (ROD) side. 3D bone morphometry showed a significant increase in bone volume (BV/TV) at UOD sites compared with ROD at 2 and 3 weeks. The average BV/TV value in the UOD group was the largest at 3 weeks and had decreased at 4 weeks (Fig. 1D). On the other hand, the BV/TV value at ROD sites gradually increased through 4 weeks.

UOD sites showed enhanced bone regeneration

Following HE staining, more regenerated tissues were observed in the UOD group than in the ROD group. The regenerated tissue was thicker and denser at the UOD sites than at the ROD sites throughout the observation period (Fig. 2). On day 0, the cut edge of the bone was smooth in UOD tissues, while it was irregular and thin in ROD tissues. After 1 week, more regenerated tissues with thickened new bone and connective tissues were observed in the bone gaps. In the UOD sites, continuous collagenous fibres with blood vessels between the wounded area and newly formed bone were found in the peripheral bone tongue of the restricted area. In the ROD sites, thinner or more amorphous collagenous tissues and blood clots were found between bone ends than in UOD.

In the sections from 2 weeks after surgery, more regenerated tissue was observed in the bone gap. New bone covered with cuboidal osteoblasts was found adjacent to the bone defect in the UOD-cut tissues

(Fig. 3A and B). Additionally, the bone cut by the ROD was covered by new bone, but the covered surface was smaller than that cut by UOD. In the regenerated tissues of the ROD sites, more inflammatory cells were scattered in the loose connective tissues. After 3 weeks, the bone end was almost covered with newly formed bone in the UOD group, while newly formed bone covered partially in the ROD group. After 4 weeks, we observed continuous new bone in the UOD group, while there was still a gap between the bone ends in the ROD group (Fig. 2A-C). Regarding the length of the bone defect, the UOD cuts were shorter than the ROD cuts at the 1^{st} and 2^{nd} weeks, suggesting that bone regeneration was faster in the UOD group. At the 3^{rd} and 4^{th} weeks, the distance tended to be shorter in the UOD group than in the ROD group, although the difference was not statistically significant (Fig. 2B). Quantitative analysis of bone thickness revealed that the bone of the UOD group was significantly thicker than that of the ROD group at the 2^{nd} week. In the UOD group, the bone thickness peaked at the 2^{nd} and 3^{rd} weeks and then decreased. In the ROD group, the thickness gradually increased from the 1^{st} week to the 4^{th} week (Fig. 2C).

UOD sites showed active osteogenesis and a weaker foreign body reaction

In the regenerated tissues at the sites of the UOD cuts after 2 weeks, many fibroblast and osteoblast clusters were observed adjacent to bone. The UOD-cut bone surface was covered by newly formed bone with more cuboidal osteoblasts on the surface of newly formed bone (Fig. 3A and B). The newly formed bone was filled with osteoblastic osteoblasts in the osteoid deposit of mineralized and unmineralized bone matrix, suggesting active bone regeneration. In addition, more osteoblasts, osteoblastic osteocytes (embedded into newly formed bone), and osteocytes were found within the newly formed bone in UOD than in ROD, which was significantly different at 1 and 2 weeks (Fig. 3A-C). The area of newly formed bone surrounding the cut bone was significantly larger in UOD than in ROD at 2 weeks (Fig. 3B). In the ROD group, cuboidal osteoblasts were found on part of the cut surface, but few were found on the side of the periosteum or the dura mater. Most osteoblasts and fibroblasts appeared to be thinner in the regenerated tissues of the ROD sites. Only in the ROD tissues the black foreign bodies of different sizes found in the granulation tissue, especially in the periosteum under the hypodermis (Fig. 3D-F). Some giant cells phagocytosing foreign bodies were distributed in the hypodermis and in the regenerated tissue (Fig. 3F). The foreign bodies are suggested to be a scattered small part of the round bur. The histomorphometric analyses of newly formed bone showed that the area in the UOD group was largest at 3 weeks, while in the ROD group, the area still increased between the 3- and 4-week time points. (Fig. 3B).

Cells obtained from bone cut with the UOD had more proliferative potential

Fewer osteoblast-like cells were obtained from ROD-cut bone chips than from UOD-cut bone chips after 14 days of culture. Harvested outgrowing osteoblast-like cells were 5.68×10^6 cells in the ROD group and 6.83×10^6 cells in the UOD group. We seeded the same number of cells (5000 cells/cm^2) and then evaluated the osteoblastic activity by ALP and VK stains (Fig. 4A) and proliferative ability (Fig. 4B). We observed significantly more osteoblastic cells in the UOD group than in the ROD group at 7 days and found that the cells from the UOD group showed greater proliferative activity than the cells from the ROD group at all observed time points.

Discussion

Ultrasonic microvibration-based bone cutting is proposed as a promising, precise system for various oral maxillofacial surgeries, including sinus lifts, bone-graft harvesting, osteogenic distraction, and dental extraction [1]. Several studies have discussed the differences in safety and efficacy between piezoelectric surgery and the traditional high-speed electric drill. Some clinical studies have shown differences in operation time [9], blood loss [10], osseointegration [11], and postoperative pain [12]. Those studies seem to assume that the UOD is a useful instrument, although it takes longer operation time. Otherwise, there has been no conclusive answer on the utility of UODs because of limitations such as the number of patients and the experimental design. Using a split rat calvarial model, in which we cut the same region of bone bilaterally in the same individual animal, we demonstrated faster healing with a larger volume of regenerated tissue and new bone formation after osteotomy with a UOD than with an ROD. In the histological and SEM observations, the margin of osteotomy was smooth in the UOD cuts and rough in the ROD cuts. Histological regenerated tissue formation showed similar processes in both ROD and UOD sites. These results are consistent with previous reports [13, 14], but they did not clearly show the superiority of ultrasonic instruments. The discrepancy between the present study and previous reports was suggested to be due to the experimental design or close histological observations.

In the regenerative process, a larger bone volume was observed in the UOD than in the ROD sites from 1 to 2 and 3 weeks after osteotomy, and the regenerated bone was more evident in the UOD sites in the reconstructed voxel views from 2 and 4 weeks than in the ROD sites. The bone volume of ROD sites showed a gradual increase from 1 to 4 weeks, while that of UOD sites peaked after 3 weeks and decreased after 4 weeks. This result suggested that bone formation of UOD tissue was maximal at approximately 3 weeks before giving way to reconstruction processes, while the bone formation process continued in the tissue of ROD sites. The results from histomorphometric analyses of the distance between cutting edges and bone thickness also supported that the period of healing process differentiates UOD from ROD cuts. In the light microscopic observation of the wound close sections, we found thicker regenerated tissues between cut bone ends on the UOD side than on the ROD side. The observation with higher magnification around bony tissues showed that there were plenty of fibroblasts and osteoblasts in the eosin-rich connective tissues surrounding newly formed bone on the UOD side, while fewer fibroblasts and osteoblasts with a flattened appearance partially covered the ROD side. Furthermore, the newly formed bone observed on the UOD side was filled with heterogeneous bone matrix filled with many cuboidal osteoblastic osteocytes, while fewer and flattened osteocytes were found on the ROD side. The appearance of a cuboid shape with round nuclei and basophilic cytoplasm is presumed to be active osteoblasts and fibroblasts synthesizing extracellular matrix. These morphological characteristics were assumed to indicate active regeneration on the UOD side compared with the ROD side. This is partially consistent with the report from the tibial bilateral rat model [14] and rabbit [8]. The discrepancy in the evaluation might be due to the lack of close and detailed histological observations.

There is accumulating evidence that mesenchymal stem cells stimulated by low-intensity ultrasound (LIPUS) increase the expression of osteogenic genes [15, 16]. Uddin and Qin [15] demonstrated elevated expression of osteogenic genes such as ALP, Runt related transcription factor 2 (RUNX2), and Osterix 24 h after LIPUS stimulation in human mesenchymal stem cells and human foetal osteoblasts. We found that the osteoblastic cells from the UOD cut had enhanced proliferation, osteogenic differentiation, and mineralization. Furthermore, we found more osteoid tissue with cuboidal osteoblasts, fibroblasts, and osteocytes in the regenerated tissues in the wound gap. It is suggested that the in vivo stimulation by UOD cut might lead mesenchymal cells to activate proliferative and osteogenic differentiation and then regenerate faster than ROD cut tissue. Chiriac et al. [17] showed that UOD cutting could maintain osteocyte health in the bone cutting zone and that the outgrown cells had osteoblastic characteristics; additionally, other researchers indicated that osteoblastic cells harvested with a UOD had high cell viability [18, 19]. We suggest that the rapid regeneration in UOD-cut tissue compared to ROD-tissue tissue occurred because ultrasound stimulation does not damage osteoblastic cells but rather preserves or even activates then.

In the ROD-cut tissue, we found many grains from the carbide bur and multinucleated giant cells filled with foreign bodies, along with other inflammatory cells. Although we carefully generated bone defects with little damage, the ROD appeared to have caused damage to the remaining tissue (e.g., dura, middle meningeal artery or vein). Curled peripheral bone ends under the observation of SEM and a larger number of inflammatory cells in the ROD tissues than in the UOD tissues suggested that UOD caused larger stress to the wounded area. Additionally, it is suggested that inflammatory cells, including multinucleated giant cells, might release inflammatory cytokines. The increased damage and induction of the inflammatory reaction might impair the regenerative capability after ROD stimulation.

The results of the present study are in agreement with the superior performance of ultrasonic treatment in previous studies [6, 17, 26]. The molecular mechanisms of this higher regenerative reaction of ultrasound treatment remain to be elucidated. Ultrasound microvibration is considered the mechanical stress to the cells [20]. Recently, Qiu et al. [21] clearly demonstrated that the mechanosensitive ion channel Piezo1 is activated by low-intensity ultrasonic stimulation and induces calcium influx in cells. Piezo1, a very large, evolutionarily conserved transmembrane protein, is one of the most sensitive channels to physical force [16]. Piezo1 has recently been demonstrated to be an essential molecule for bone formation [22]. Piezo channels are reported to function not only osteoblasts but also mesenchymal cells [23], human dental pulp cells [24], and endothelial cells [25]. It is suggested that low-intensity ultrasonic stimulation by a UOD activates Piezo1 of the plasma membrane of mesenchymal or osteoblastic cells and surrounding cells, potentially speeding the regeneration process. Further studies are needed to clarify the mechanisms of the tissue reaction and longer consequences.

In conclusion, the results of the present study provide in vivo evidence that bone heals more quickly if cut with a UOD than with an ROD. Our in vitro experiments demonstrated that the cells from the UOD cuts had higher proliferative activity than those from the RODs cut. We suggest here that ultrasonic osteotomy is a

preferable option in the surgeries needed for early bone augmentation, such as dental implants with bone grafts.

Methods

Animals

All experimental procedures were reviewed and approved by the Saga University Animal Care and Use Committee (number: 26-051-0) and were performed in accordance with the regulations on animal experimentation at Saga University.

We used 6-week-old male Wistar rats (Jcl: Wistar, outbred, no genetic modification) weighing 198.8-212.2 g (Kyudo Corporation, Tosu, Japan). Animals were acclimated a week before surgery and were housed with food and water *ad libitum* under specific pathogen-free conditions. Three animals were bred in each cage. Fifteen animals were used for micro-CT and histological analyses, 3 animals were used for scanning electron microscopy (SEM), and another 3 animals were used for in vitro experiments. The total number of animals used was 21. Since at least 3 animals were required for each experiment and each timepoint and 5 timepoints were required to evaluate bone healing, the minimum number of animals was adopted, in consideration of animal ethics. All animals met the appropriate conditions because the species, sex, age, and weight of the animals were almost the same. In addition, no animals were excluded from the analysis during the experiments because no adverse events occurred. They were anaesthetized intraperitoneal injections with 3 mixed anaesthetic agents (0.4 mg/kg dexmedetomidine hydrochloride, 2.0 mg/kg midazolam and 5.0 mg/kg butorphanol tartrate) and subcutaneous anaesthesia to the head by 2% lidocaine with 1/80,000 epinephrine (Showa Yakuhin Kako, Tokyo, Japan). We adhered to the Animal Research: Reporting of *In Vivo* Experiments (ARRIVE) guidelines and Japanese guidelines in conducting these animal experiments.

Osteotomy devices

For ultrasonic osteotomy, VarioSurg3® with a titanium nitride coating H-SG1 tip (Blade width 0.6 mm) (NSK, Tochigi, Japan) was used with a driving frequency of 30 kHz and an output power of 17 kW (average) under saline irrigation. The tip was the most frequently used in clinical cases, and it could cut a calvarial bone defect in a few strokes. For conventional rotary osteotomy, we used a Surgic Pro® (NSK, Tochigi, Japan) with a round bur with a 0.8-mm diameter (Komet, SC, USA) at 40,000 rpm and 80 N/cm under saline irrigation. The round bur used was able to cut the bone defect set in the same way as the UOD tip with a few strokes.

Osteotomy design and operation procedure

After the head hair was shaved, an incision was made into the scalp under the local and general anaesthesia mentioned above. Before cutting, the cutting line of the osteotomy was marked with a pencil

using a template made of resin. We utilized a craniotomy design consisting of pairs of cuts described by Anesi et al. [26].

For the bone healing evaluation by micro-computed tomography (CT) and histology, we made an 8 × 2-mm bone defect in the right calvaria with a UOD and a bone defect of the same size in the left calvaria with an ROD. During the ROD cut, we took care not to damage the dura with the instruments. A square 8 8-mm osteotomy was used for surface morphological analysis by SEM. The wounds were irrigated after bone cutting and closed by 4-0 silk threads. The cutting time for each appliance was recorded. After surgery, meloxicam (Fujifilm Wako Pure Chemical Corporation, Osaka, Japan) was intramuscularly injected at 0.2 mg/kg. After the surgery, the rats were given drinking water mixed with antibiotics (cefaclor monohydrate, 10 mg/kg body weight, Fujifilm Wako Pure Chemical Corporation, Osaka, Japan) for two days. Specimens were collected immediately after the operation (0 days) and 1, 2, 3 and 4 weeks later for micro-CT three-dimensional bone morphology measurements and for histological evaluation by haematoxylin-eosin (HE) staining.

Micro-CT analysis

Animals were euthanized by deep anaesthesia at 0 days and 1, 2, 3 and 4 weeks after surgical osteotomy. Three rats at each time point, 15 animals in total, were used in the experiment. Three animals were bred in each cage, and upon evaluation, the animals in randomly selected cages were selected and analysed to minimise potential confounders. After euthanization, the whole calvaria was removed carefully with surgical scissors to avoid damaging the defective area. Tissue samples were fixed with 4% paraformaldehyde for 24 h and rinsed with 0.1 M phosphate buffered saline and then acquired images by micro-CT (MCT-CB130, Hitachi Medical Corporation, Tokyo, Japan: tube voltage; 60 kV, tube current; 100 μA) followed by three-dimensional bone morphometry using TRI/3D-BON software (Ratoc Engineering, Tokyo, Japan). The parameters measured were BV/TV, which indicates the bone volume in total tissues in the region of interest (ROI). The ROI had a size of 150×280×100 voxels centred on the bone defects. The voxel size was 26 μm. The evaluator performed the analysis without knowing whether the bone defect had been made with a UOD or an ROD.

Histological analysis

After micro-CT evaluation, samples were decalcified in 10% ethylenediaminetetraacetic acid (EDTA) tetrasodium tetrahydrate solution for one week, dehydrated through ascending alcohol concentrations, paraffin embedded and sectioned 8 μm thick. The sections were then dewaxed and processed for HE staining for light microscope analysis. The osteotomy gap width of the two native bone surfaces surrounding the osteotomy was evaluated in the section around the middle of the wound using ImageJ software [27]. The distance was measured at 2 points, and the average was evaluated.

SEM observation

To determine the structural difference between the UOD cut and the ROD cut, we collected bones from 3 rats in each group just after ostectomy. Specimens were fixed with 4% paraformaldehyde (Sigma-Aldrich, St Louis, MO, USA) with 2.5% glutaraldehyde (Sigma-Aldrich, St Louis, MO, USA) in 0.2 M phosphate buffer, pH 7.4, for 24 h at 4°C. After rinsing with 0.2 M phosphate buffer (PBS), the specimens were fixed with 1% osmium oxide for 24 h at 4°C, dehydrated and freeze-dried with t-butyl alcohol (2-methyl-2-propanol). The dried specimens were coated with platinum, and the surface morphology was examined by SEM (JSM-6510, JEOL, Tokyo, Japan).

Isolation and cultivation of osteoblast-like cells

After being cut with an ROD or a UOD, the calvarial bone was extracted, and 8 8 mm bone blocks were further divided into two pieces. Primary osteoblast-like cells were isolated according to a protocol by Frosch et al. [28]. The bone blocks were rinsed with 0.1 M PBS three times and placed on 35-mm cell culture dishes (BD Falcon, NJ, USA), covered with 0.5 ml culture medium and incubated at 37°C in a 100% humidified incubator containing an atmosphere of 95% air and 5% carbon dioxide. The culture medium was alpha MEM (Fujifilm Wako Pure Chemical Corporation, Osaka, Japan) supplemented with 10% foetal bovine serum (FBS) (Sigma-Aldrich, St. Louis, MO, USA) and streptomycin, penicillin and amphotericin B. After 30 minutes, another 1 ml of culture medium was added. After two weeks of culture, the cells were gently rinsed with 0.1 M PBS and incubated with 0.05% trypsin/EDTA (GIBCO, NY, USA). After being counted, the cells were resuspended and seeded in 60-mm culture dishes (BD Falcon, NJ, USA). After reaching confluence, cells were resuspended and seeded in 100-mm dishes (BD Falcon, NJ, USA) and used for the cell proliferation assay. In this experiment, 6 rats were used (3 in each group).

Cell proliferation assay

Cells were seeded into 96-well plates at 5000 cells/cm^2, and cell counts were measured by colorimetry assay at 450 nm (Cell Counting Kit-8, Dojindo, Kumamoto, Japan) for 24, 48, 72, 120 (5 days) and 168 h (7 days). The medium was changed every 72 h. Experiments were performed in triplicate.

Cell differentiation assay (alkaline phosphatase and von Kossa staining)

Cells were re-seeded into 24-well plates at 5000 cells/cm^2 in the culture medium. After 24 h, the same cells were stimulated with an osteoinduction medium consisting of 10% FBS, 50 μg/ml ascorbic acid, and 5 mM β-glycerophosphate. The medium was changed every 3 days. The cells were fixed and stained with alkaline phosphatase (ALP) stain at day 14 and von Kossa (VK) stain at day 28.

Statistical analysis

Statistical analyses were performed using JMP ver.14.0 software (SAS Institute Inc., NC, USA). One-way ANOVA was used for 3D and 2D bone morphometry. Student's *t*-test was used to assess cell proliferation. p values of <0.05 indicated significant differences between the groups.

Declarations

ACKNOWLEDGMENTS

We appreciate the technical support from the Analytical Research Center for Experimental Sciences Saga University.

DECLARATIONS OF INTEREST

None of the authors received any personal fees or non-financial support.

FUNDING

This work was supported by a Kakenhi Grant-in-Aid for Challenging Exploratory Research (20K21683). This study was also partly supported by the Nakanishi incorporated. Shin-ichi Tanaka, an employee of Nakanishi Incorporated, set the experimental conditions in this study, and he is an expert on the mechanisms of the devices.

ACKNOWLEDGEMENTS

We appreciate the technical support from the Analytical Research Center for Experimental Sciences Saga University.

ROLE OF THE FUNDING SOURCE

This work was supported by a Kakenhi Grant-in-Aid for Challenging Exploratory Research (20K21683). This study was also partly supported by the Nakanishi incorporated. Shin-ichi Tanaka, an employee of Nakanishi Incorporated, set the experimental conditions in this study, and he is an expert on the mechanisms of the devices.

ETHICAL APPROVAL

This study adhered to the Animal Research: Reporting of *In Vivo* Experiments (ARRIVE) guidelines in reporting on the study design and statistical analysis, experimental procedures, experimental animals, and animal housing and husbandry.

DATA AVAILABILITY

The datasets generated during and/or analysed during the current study are available from the corresponding author on reasonable request.

AUTHOR CONTRIBUTIONS STATEMENT

Atsushi Danjo: Design of the work, Data acquisition, Analysis, Interpretation of the data, Drafted the work

Reona Aijima: Data acquisition, Analysis

Reiko U. Yoshimoto: Data acquisition, Analysis

Shin-Ichi Tanaka: Design of the work, Analysis

Takeshi Katsushi: Conceptualization, Interpretation of the data

Mizuho A. Kido: Funding acquisition, Interpretation of data, Writing-Review and Editing

Yoshio Yamashita: Funding acquisition, Interpretation of data, Writing-Review and Editing

References

1. Pavlíková, G. *et al.* Piezosurgery in oral and maxillofacial surgery. *Int J Oral Maxillofac Surg.* **40**, 451–457(2011).
2. Barone, A. *et al.* A randomized clinical evaluation of ultrasound bone surgery versus traditional rotary instruments in lower third molar extraction. *J Oral Maxillofac Surg.* **68**, 330–336(2010).
3. Silva R, Gupta R, Tartaglia G, Connelly S. Benefits of using the ultrasonic BoneScalpel™ in temporomandibular joint reconstruction. *J Cranio Maxillofac Surg.* **45**, 401–407(2017).
4. Li, K. *et al.* Safety and efficacy of cervical laminoplasty using a piezosurgery device compared with a high-speed drill. **95**, e4913(2016).
5. Kokuryo, S. *et al.* Comparison of the effects of ultrasonic and conventional surgery on the neurosensory disturbance after bilateral sagittal split osteotomy. *J Oral Maxillofac Surg*. **76**, 1539–1545(2018).
6. Vercellotti, T. *et al.* Osseous response following resective therapy with piezosurgery. *Int J Periodontics Restor Dent.* **25**, 543–549(2005).
7. Jung, Y.J. *et al.* Focused low-intensity pulsed ultrasound enhances bone regeneration in rat calvarial bone defect through enhancement of cell proliferation. *Ultrasound Med Biol.* **41**, 999–1007(2015).
8. Ma, L. *et al.* Wound healing of osteotomy defects prepared with piezo or conventional surgical instruments: a pilot study in rabbits. *J Investig Clin Dent.* **6**, 211–220(2015).
9. Al-Moraissi, E.A. *et al.* Does the piezoelectric surgical technique produce fewer postoperative sequelae after lower third molar surgery than conventional rotary instruments? A systematic review and meta analysis. *Int J Oral Maxillofac Surg.* **45**, 383–391(2016).
10. Pagotto, L.E.C. *et al.* Piezoelectric versus conventional techniques for orthognathic surgery: systematic review and meta-analysis. *J Cranio Maxillofac Surg.* **45**, 1607–1613(2017).
11. Canullo, L. *et al.* Piezoelectric vs. conventional drilling in implant site preparation: pilot controlled randomized clinical trial with crossover design. *Clin Oral Implants Res.* **25**, 1336–1343(2014).
12. Tekdal, G.P., Bostanci, N., Belibasakis, G.N., Gürkan, A. The effect of piezoelectric surgery implant osteotomy on radiological and molecular parameters of peri-implant crestal bone loss: a randomized, controlled, split-mouth trial. *Clin Oral Implants Res.* **27**, 535–544(2016).

13. Esteves, J.C. *et al.* Dynamics of bone healing after osteotomy with piezosurgery or conventional drilling - histomorphometrical, immunohistochemical, and molecular analysis. *J Transl Med.* **11**, 221(2013).
14. Reside, J. *et al.* In vivo assessment of bone healing following piezotome® ultrasonic instrumentation. *Clin Implant Dent Relat Res.* **17**, 384–394(2015).
15. Uddin, S.M.Z., Qin, Y.X. Enhancement of osteogenic differentiation and proliferation in human mesenchymal stem cells by a modified low intensity ultrasound stimulation under simulated microgravity. *PLoS One.* **8**, e73914(2013).
16. Costa, V. *et al.* Osteogenic commitment and differentiation of human mesenchymal stem cells by low-intensity pulsed ultrasound stimulation. *J Cell Physiol.* **233**, 1558–1573(2018).
17. Chiriac, G. *et al.* Autogenous bone chips: influence of a new piezoelectric device (PiezosurgeryR) on chip morphology, cell viability and differentiation. *J Clin Periodontol.* **32**, 994–999(2005).
18. von See, C. *et al.* Comparison of different harvesting methods from the flat and long bones of rats. *Br J Oral Maxillofac Surg.* **48**, 607–612(2010).
19. Pereira, C.C.S. *et al.* Comparative evaluation of cell viability immediately after osteotomy for implants with drills and piezosurgery. *J Craniofacial Surg.* **29**, 1578–1582(2018).
20. Ozcivici, E. *et al.* Mechanical signals as anabolic agents in bone. *Nat Rev Rheumatol.* **6**, 50–59(2010).
21. Qiu, Z. *et al.* The mechanosensitive ion channel piezo1 significantly mediates in vitro ultrasonic stimulation of neurons. **21**, 448–457(2019).
22. Sun, W. *et al.* The mechanosensitive piezo1 channel is required for bone formation. **8**, e47454(2019).
23. Sugimoto, A. *et al.* Piezo type mechanosensitive ion channel component 1 functions as a regulator of the cell fate determination of mesenchymal stem cells. *Sci Rep.* **7**, 17696(2017).
24. Gao, Q., Cooper, P.R., Walmsley, A.D., Scheven, B.A. Role of piezo channels in ultrasound-stimulated dental stem cells. *J Endod.* **43**, 1130–1136(2017).
25. Morley, L.C. *et al.* Piezo1 channels are mechanosensors in human fetoplacental endothelial cells. *Mol Hum Reprod.* **24**, 510–520(2018).
26. Anesi, A. *et al.* Structural and ultrastructural analyses of bone regeneration in rabbit cranial osteotomy: piezosurgery versus traditional osteotomes. *J Cranio Maxillofac Surg.* **46**, 107–118(2018).
27. Schneider, C.A., Rasband, W.S., Eliceiri, K.W. NIH image to imageJ: 25 years of image analysis. *Nat Methods.* **9**, 671–675(2012).
28. Frosch, K.H. *et al.* Migration, matrix production and lamellar bone formation of human osteoblast-like cells in porous titanium implants. *Cells Tissues Organs.* **170**, 214–227(2002).

Figures

A

Device	Average osteotomy time (sec)
UOD	66.6 ± 17.8**
ROD	23.9 ± 7.9

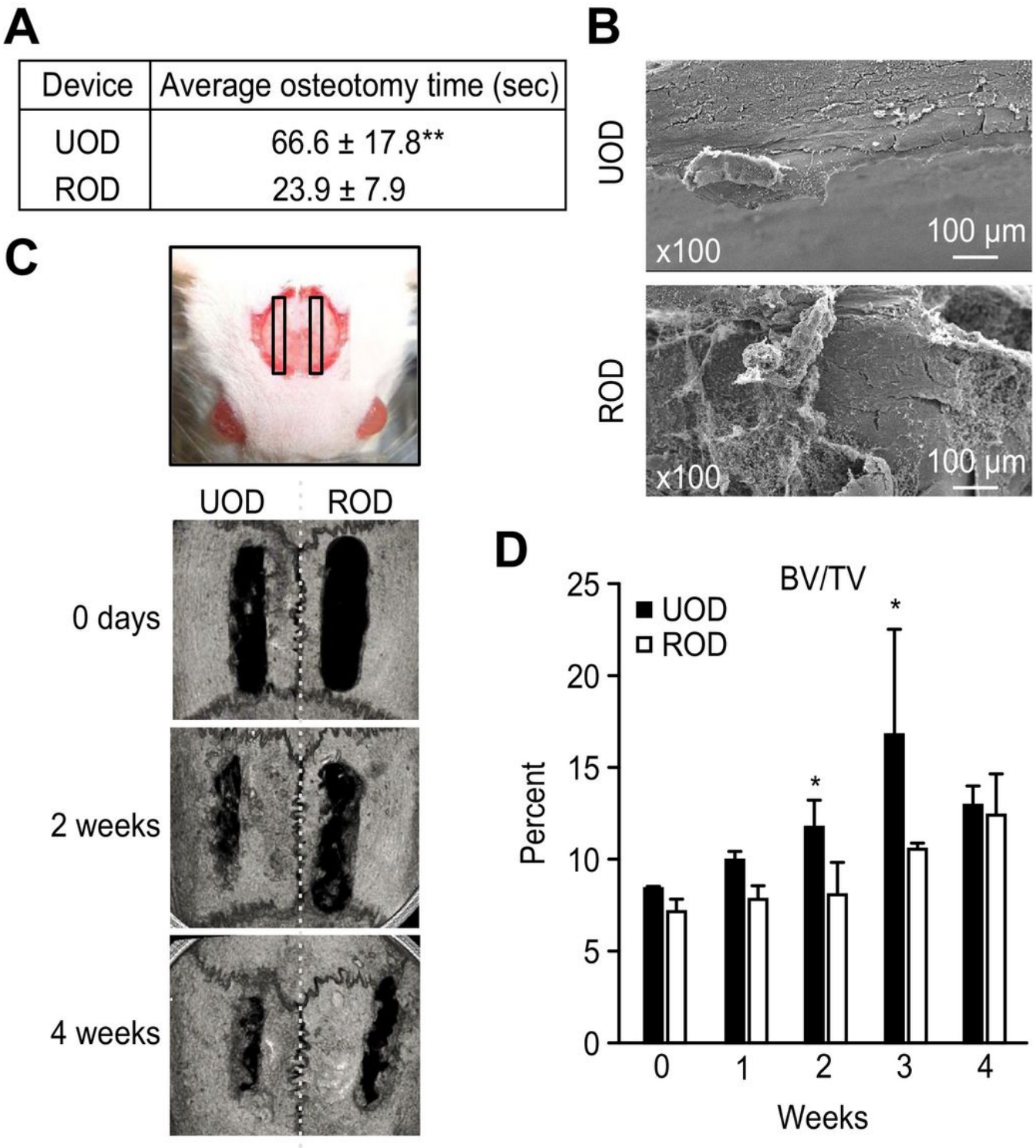

Figure 1

A: Comparison of osteotomy time. The ROD was significantly faster than the UOD by approximately 2.8 times. **: p<0.01. B: SEM micrographs showing the cutting surfaces made by the UOD (upper) and the ROD (lower). Scale bar= 100 μm. C: Scout views of micro-CT of calvaria after 0 days and 2 or 4 weeks after osteotomy. The uppermost box shows the osteotomy design of the split model. The left defects in the rat calvaria were made by UOD, and the right defects were made by ROD. D: Changes in BV/TV in the

UOD group (black bars) and the ROD group (white bars). The volume of new bone (BV/TV) was greater in the UOD group than in the ROD group at 2 and 3 weeks. n=3. *: p<0.05.

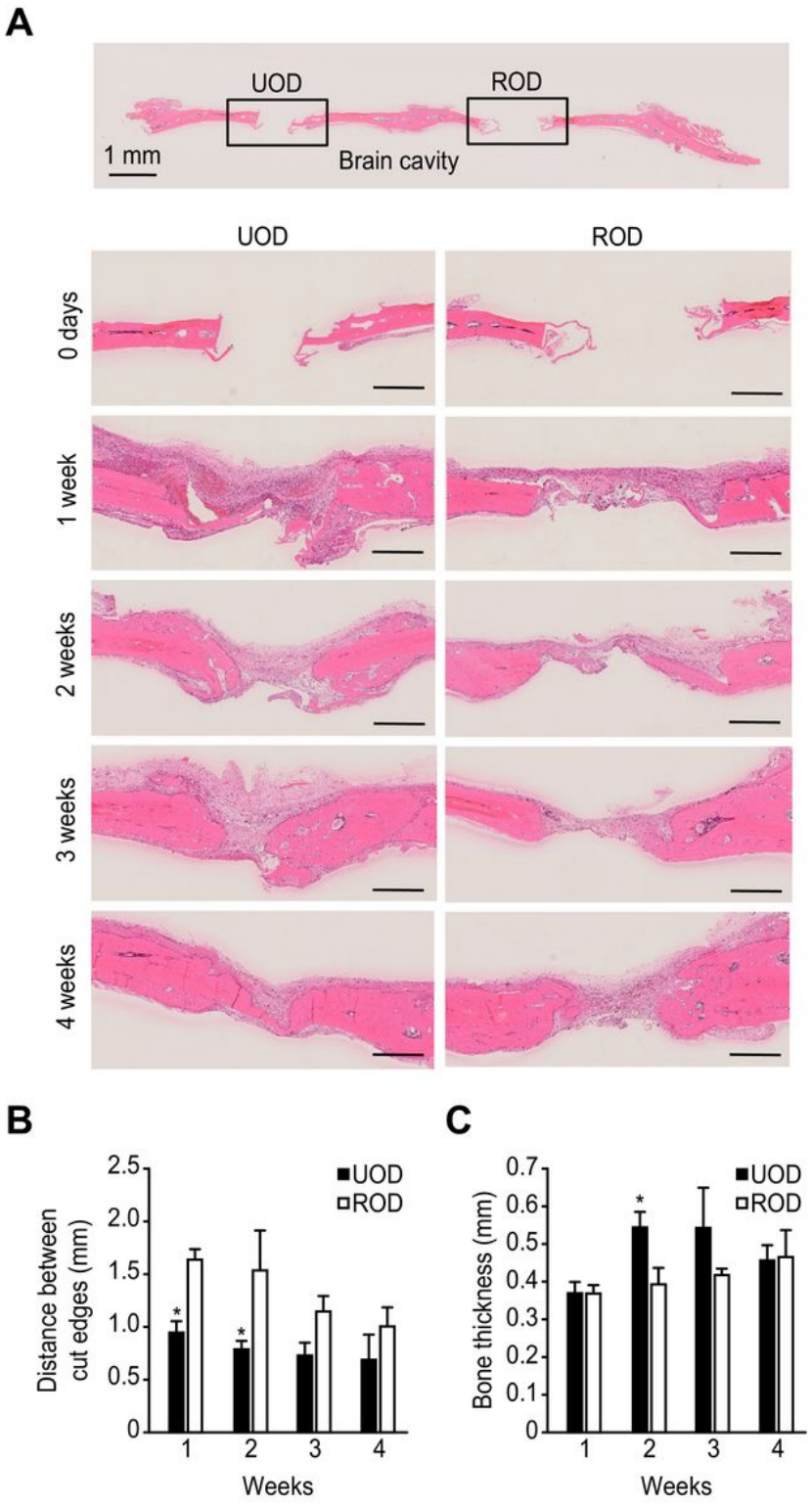

Figure 2

A: Coronal section of the calvarial tissue cut by the UOD (left) and the ROD (right) at 0 days and 1, 2, 3 and 4 weeks after surgery. HE staining. Scale bars= 100 μm. The uppermost micrograph shows the calvaria at a lower magnification as of day 0. The box indicates the area shown at a higher magnification

below. The thickness of the regenerated tissue in the wound was different between the UOD and ROD groups. B: Changes in the distance between wound edges from 1 w to 4 w in the UOD group (black bars) and in the ROD group (white bars). n=3. *: p<0.05. C: Changes in bone thickness from 1 w to 4 w in the UOD group (black bars) and in the ROD group (white bars). n=3. *: p<0.05.

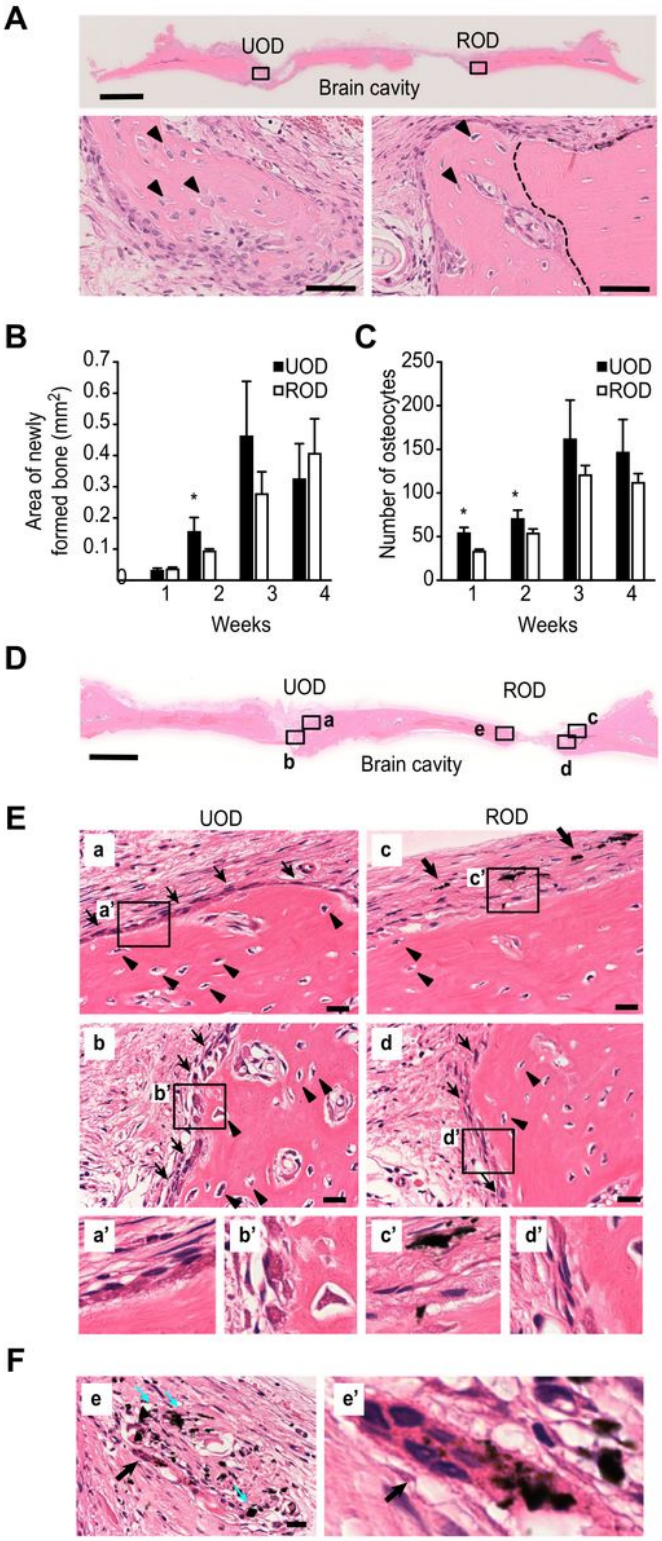

Figure 3

A: Micrographs of rat calvarial tissue at 2 weeks. The arrowheads indicate osteocytes found in the newly formed bone. The margin of the original bone and the edge of the defect are indicated by dotted lines. HE staining was used. Note the regenerated bone at the UOD cutting site, with clusters of osteoblasts and fibroblasts in osteoid tissue with divergent eosin staining (left), while the ROD cutting site (right) has uniformly eosin-stained osteoid tissue covered in a thin layer of osteoblasts. Scale bars= 1 mm (low magnification) and 50 μm (high magnification). B: Summary of newly formed bone area at the UOD cutting site (black bars) and the ROD cutting site (white bars). n=3. *: $p<0.05$. C: Number of osteocytes in newly formed bones at the UOD cutting site (black bars) and the ROD cutting site (white bars). n=3. *: $p<0.05$. D: Low-magnification image of rat calvarial tissue at 3 weeks. Scale bar =1 mm. E: High-magnification images of section from the UOD (left) and ROD cutting sites (right) at 3 weeks. A magnified image of boxes (a, c) in (D) shows the area around the periosteum, and a magnified image of boxes (b, d) in (D) shows the edge of the cut. Arrows and arrowheads indicate cuboidal osteoblasts and osteocytes, respectively, in the newly formed bone. Insets (a'–d') show higher-magnification views of the osteoblasts in the black boxes in each image. Thick arrows in the ROD group indicate foreign bodies scattered in the tissue. Scale bars= 20 μm. F: High magnification image of the box (e) in (D) shows a giant cell filled with a foreign body (thick arrow, inset), as well as foreign bodies (blue arrows) within the connective tissue at the ROD cutting site. Scale bar= 20 μm.

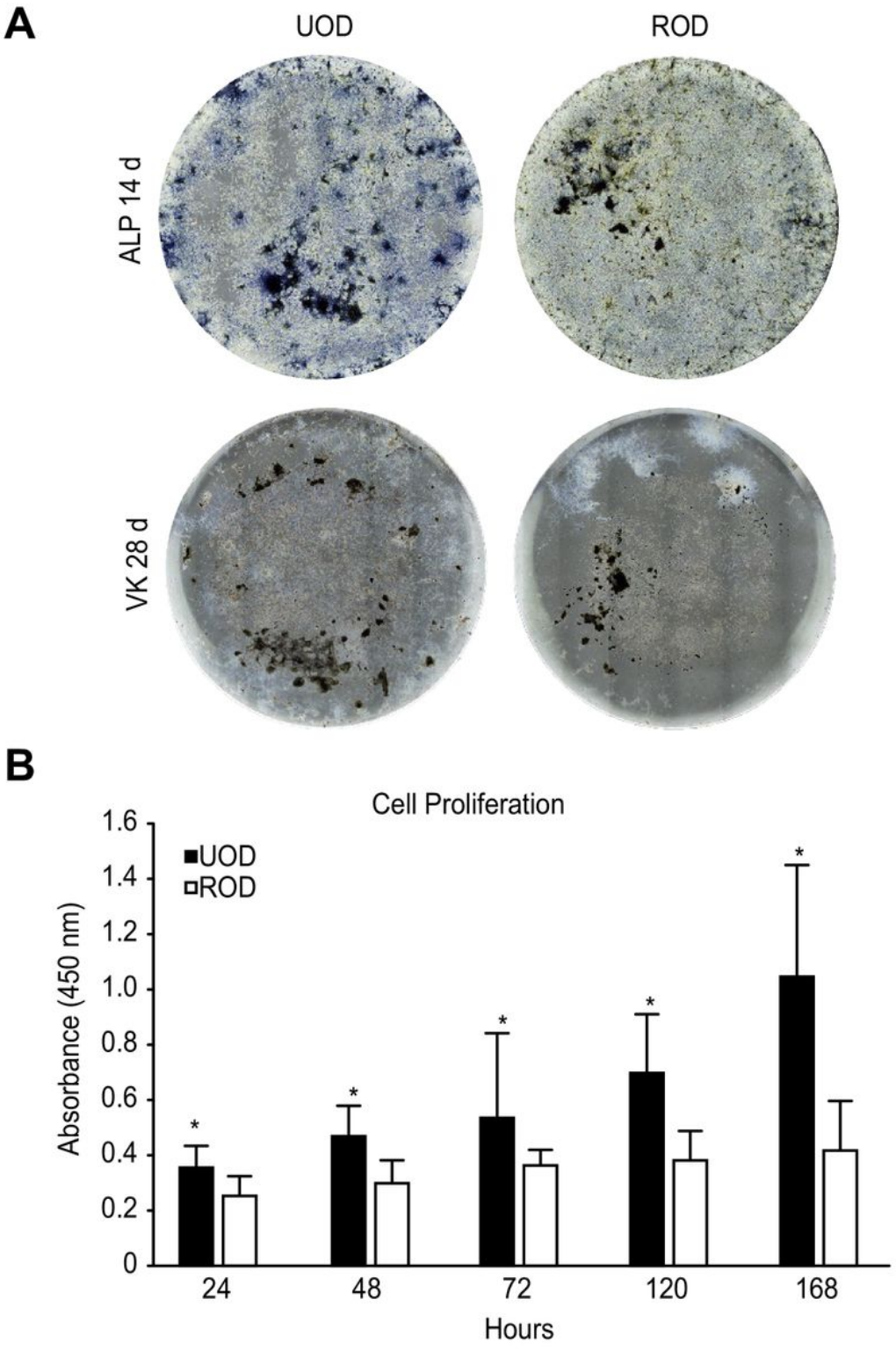

Figure 4

A: Representative image of alkaline phosphatase (ALP) staining (upper row) on day 14 of culture and von Kossa (VK) staining (lower row) on day 28 of culture in cells from the UOD group (left) and ROD group (right). B: Summary of the cell proliferation assay using outgrown osteoblastic cells from bone chips derived from the UOD group (black bars) or the ROD group (white bars) at 24, 48, 72, 120, and 168 h. n=3. *: $p<0.05$.